12

Off-line model predictive control of dc-dc converter

Tadanao Zanma and Nobuhiro Asano
Mie University
Japan

1. Introduction

Control systems with switching modes in which different dynamics are assigned are called hybrid dynamical systems and are being actively researched (1–6). The continuous behavior in the hybrid dynamical system is expressed generally by differential or difference equations, while the discrete behavior is described by logics or state machines such as automata. If a system can be regarded as a hybrid dynamical system, both continuous and discrete properties can be dealt with concurrently. Therefore, a hybrid dynamical system has the ability to represent many systems as a single model without dividing into separate continuous and discrete systems.

Power electronic circuits can also be regarded as hybrid dynamical systems as they share both continuous and discontinuous behaviors(7–14). The continuous behavior of current or voltage in such a system is subject to passive elements such as resistance, capacitance and inductance, whereas the discontinuous element of switching devices such as MOSFETs and IGBTs yields an on-off signal that is essentially discrete.

A conventional method currently being used for the control of dc-dc converters is PWM (Pulse Width Modulation) with triangular wave. The average output voltage is controlled by PWM, which determines on-off switching timing by employing relatively high carrier frequency. However, the reference may vary in the half period of triangular wave carrier if the carrier frequency is lowered to decrease switching loss for saving energy. Then, the average voltage can no longer approximate the voltage reference. One possible reason is that the control frequency is determined by the carrier frequency only. Another reason may be that the PWM method focuses only on the average output characteristic and excludes switching property. Therefore, a novel method is desired for dc-dc converters by considering switching property explicitly as hybrid dynamical systems.

For synthesis of the hybrid dynamical system, various approaches have been proposed. Specifically, modeling and synthesis based on mixed logical dynamical (MLD) systems has much potential since the formulation is similar to the linear discrete time state space representation(19). The solution of the design is obtained by solving an optimization problem with the help of model predictive control (MPC)(16; 17). It derives the optimal input to minimize an estimation of a given cost function by predicting controlled variables for an MLD system. Specifically, the problem is reduced to a mixed-integer linear or quadratic programming (MILP or MIQP) problem. The method is expected to achieve better control performance than that achieved by conventional methods when applied to the output control of a power

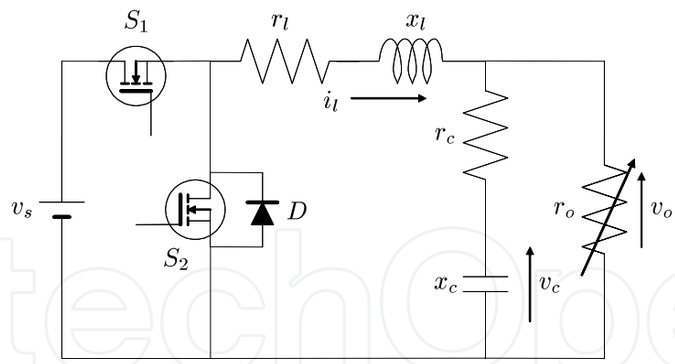

Fig. 1. Topology of the step-down dc-dc converter.

converter. However, it is difficult to solve the optimal problem online because of the computation burden caused by the control period of power converters being considerably short compared to that in mechanical or process control systems.
This paper proposes a control method using the MPC for the output control problem of the dc-dc converter. The considered system is described as an MLD system form. In our work(14), one control period is divided into N submodels. Thus, additional auxiliary variables are needed. In addition, the state variable among the submodels is handled as an averaged one. The method in this paper, however. requires no averaging. The explicit switching law is given as a direct gate signal for the switching devices. Moreover, it is emphasized that a quadratic cost function which was not adopted in a previous work(14) is addressed in this paper so that not only the tracking error but also the switching losses can be considered. The proposed control method achieves quick tracking to the reference in transient state, while keeping the switching frequency as small as possible in steady state. To verify the effectiveness of the proposed method, numerical simulations and experimental results are illustrated.
This paper is organized as follows. In Section 2, a step-down dc-dc converter and MLD system are introduced. Next, the optimization problem for the control is described. Following several simulation results, Section 3 proposes a modified control method taking into account the computation delay. Then, experimental results are shown in Section 4. Finally, Section 5 concludes this paper. In the Appendix, formulation of constraints and transformation to mp-MIQP are explained.

2. Preliminaries

In this section, a step-down dc-dc converter is considered as an example of power electronic circuits. After the formulation, an MLD system(19) and multi-parametric MIQP (mp-MIQP)(18) are reviewed.

2.1 Step-down dc-dc converter

The circuit topology of the step-down dc-dc converter is shown in Fig. 1. The dc-dc converter controls the load voltage v_o with on-off switches S_1 and S_2. The resistance r_o expresses the load. The equivalent series resistance of the capacitor and the internal resistance of the inductor are denoted by r_c and r_l, respectively, while x_l and x_c represent inductance and capacitance of the low-pass filtering stage, respectively. Switches S_1 and S_2 cannot be conducted simultaneously. Together with diode D, switch S_2 provides a path for the inductor current i_l

regardless of whether it is positive or negative. The continuous time state-space representation of the dc-dc converter shown in Fig. 1 is given by

$$\dot{x}(t) = A_c x(t) + B_c u(t), \tag{1}$$
$$y(t) = C_c x(t), \tag{2}$$

where $x(t) = \begin{bmatrix} i_l(t) & v_o(t) \end{bmatrix}'$. Denoted by $i_l(t)$ and $v_o(t)$ are the inductor current and output voltage, respectively. The matrices A_c, B_c and C_c are given by $A_c = \begin{bmatrix} -\frac{r_l}{x_l} & -\frac{1}{x_l} \\ \frac{r_o}{r_c+r_o}(\frac{1}{x_c} - \frac{r_c r_l}{x_l}) & -\frac{r_o}{r_c+r_o}(\frac{1}{x_c r_o} + \frac{r_c}{x_l}) \end{bmatrix}$, $B_c = \begin{bmatrix} \frac{1}{x_l} \\ \frac{r_c r_o}{x_l(r_c+r_o)} \end{bmatrix}$ and $C_c = \begin{bmatrix} 0 & 1 \end{bmatrix}$, respectively. Eqs. (1) and (2) are sampled by T_s. Hereafter, the discrete time is described anew as t. Thus, the considered system is recast as follows.

$$x(t+1) = Ax(t) + Bu(t), \tag{3}$$
$$y(t) = Cx(t), \tag{4}$$

where $A = e^{A_c T_s}$, $B = \int_0^{T_s} e^{A_c \tau} d\tau B_c$ and $C = C_c$. Note that the value of input is limited to either 0 or v_s, which can be rewritten as follows.

$$(\forall t)\ u(t) \in \{0, v_s\}. \tag{5}$$

2.2 Representation by MLD system(19)

A mixed logical dynamical (MLD) system is described by a linear dynamical equation with linear mixed-integer inequalities so that discrete properties included in the process can be introduced into the system using logical variables. One advantage is that the logical formula can be described with linear inequalities and model predictive control can be applied.
The model of the dc-dc converter is rewritten to the MLD system representation. The auxiliary δ of 0-1 variable is introduced as a new input variable to describe the discrete variable. The variable is associated as follows.

$$[\delta(t) = 1] \rightarrow [z(t) = v_s], \tag{6}$$
$$[\delta(t) = 0] \rightarrow [z(t) = 0], \tag{7}$$

where $z(t)$ is,

$$0 \leq z(t) \leq v_s. \tag{8}$$

Eqs. (6) and (7) indicate that $z(t) = v_s$ if $\delta(t) = 1$, whereas $z(t) = 0$, otherwise. By replacing Eqs. (6) and (7) with their equivalent linear inequalities,

$$E_1\delta(t) + E_2 z(t) \leq E_3 u(t) + E_4 x(t) + E_5, \tag{9}$$

where,

$$E_1 = \begin{bmatrix} 0 & v_s & -v_s & 0 \end{bmatrix}', \tag{10}$$
$$E_2 = \begin{bmatrix} 1 & -1 & 1 & -1 \end{bmatrix}', \tag{11}$$
$$E_3 = E_4 = O, \tag{12}$$
$$E_5 = \begin{bmatrix} v_s & 0 & 0 & 0 \end{bmatrix}'. \tag{13}$$

is obtained. Inequality (9) reflects that $z(t) = v_s$ if $\delta(t) = 1$ whereas $z(t) = 0$ if $\delta(t) = 0$. Namely, $\delta(t)$ can be considered as the state of the switch: $\delta(t) = 1$ if the switch is on, $\delta(t) = 0$ otherwise. Note that $z(t)$ in inequality (8) is an apparent continuous auxiliary variable.
As a result, Eqs. (3), (4) and (5) can be transformed into an MLD system consisting of one standard linear discrete time state space representation and linear inequalities associated with the constraints on the system,

$$x(t+1) = Ax(t) + Bz(t), \tag{14}$$

$$y(t) = Cx(t), \tag{15}$$

$$\text{subject to Eq. (9).} \tag{16}$$

2.3 Multi-parametric MIQP(18)

Multi-parametric MIQP (mp-MIQP) is a type of MIQP(18) parameterized by multiple parameters. The mp-MIQP parameterized by state x of the system is described as follows.

$$\min_{\nu} \ \nu' H \nu + 2x' F \nu + x' Y x + 2C_f \nu + 2C_x x, \tag{17}$$

$$\text{subject to } G\nu \leq W + Ex, \tag{18}$$

where ν is

$$\nu = \begin{bmatrix} \Delta' & \Xi' \end{bmatrix}', \tag{19}$$

$$\Delta = \begin{bmatrix} \delta_0 & \cdots & \delta_{N_p-1} \end{bmatrix}', \tag{20}$$

$$\Xi = \begin{bmatrix} z_0 & \cdots & z_{N_p-1} \end{bmatrix}'. \tag{21}$$

In Eqs. (20) and (21), the predictive horizon in MPC is denoted by N_p.
If solved, the optimal solution of mp-MIQP is given as the piece-wise affine state feedback form. Namely, the explicit control law parameterized by the state x is obtained as follows.

$$\nu = K_i x + h_i \quad \text{if } x \in X_i, \tag{22}$$

where X_i ($i = 1, 2, \ldots$) are regions partitioned in the state space, and K_i and h_i are the corresponding constant matrices and vectors, respectively. As Eq. (22) is available off-line, the optimal input is determined online according to the state measured at each sampling.

3. Numerical simulation and revision of control method

In this section, the effectiveness of the method proposed in the previous section and the Appendix is shown by applying it to the output control of the dc-dc converter shown in Fig. 1. The control objective is to achieve quick tracking to the reference in transient state with minimal switching in steady state. For the purpose, mp-MIQP is exploited.

3.1 Simulation condition and state partition

The circuit and control parameters for simulation are listed in Tables 1 and 2, respectively.
Let us consider Eqs. (14) to (16) as the model for the dc-dc converter shown in Fig. 1. In Eq. (45), $\tilde{H}$ and L are first set as zeros. Then, the setting of these matrices imply that focus is only on tracking performance. The state partition obtained by off-line model predictive control, (mp-MIQP) and its enlarged view are shown in Fig. 2. In each region of Fig. 2, the optimal input sequence is assigned. The figure of state partition shown in Fig. 2 is generated

Table 1. Circuit parameters

source voltage v_s	5.0 [V]
inductance x_l	20 [μH]
internal resistance r_l	25 [mΩ]
capacitance x_c	2.2 [mF]
equivalent series resistance r_c	60[mΩ]
load resistance r_o	1[Ω]

Table 2. Control parameters

control period T_s	10 [μs]
predictive horizon N_p	1, 3, 5
upper limit $i_{l,\max}$	8.0 [A]
reference value v_{ref}	2.0 [V]

using of Multi-Parametric Toolbox(20). In Fig. 2, the number of state partitions is limited to at most 2^{N_p}. Each partition is specified by linear inequalities. In each partition, the solution of mp-MIQP given by Eq. (22) is assigned. To investigate to which partition it belongs, the state $\begin{bmatrix} i_l & v_o \end{bmatrix}'$ at each sampling can be performed simply since the obtained state partition is constructed by linear inequalities. Focus on the white region at the right bottom corner in Fig. 2. Whenever the state $\begin{bmatrix} i_l & v_o \end{bmatrix}'$ enters the region, switch S_1 shown in Fig. 1 is forced to turn off since the constraint about the inductor current given by Eq. (37) can no longer be satisfied.

3.2 Consideration of delay for computation of state distinction

Figs. 3 and 4 show simulation results for $N_p = 3$ and $N_p = 5$, respectively. Note that the method described in the Appendix is utilized for each of the calculations. Figs. 3 and 4, also indicate that the output voltage is kept at the specified value 2.0 [V] in steady state, while the inductor current does not exceed its limit of 8[A]. In the simulation, the computation time of state distinction for optimal input is assumed to be negligible. Little difference exists between

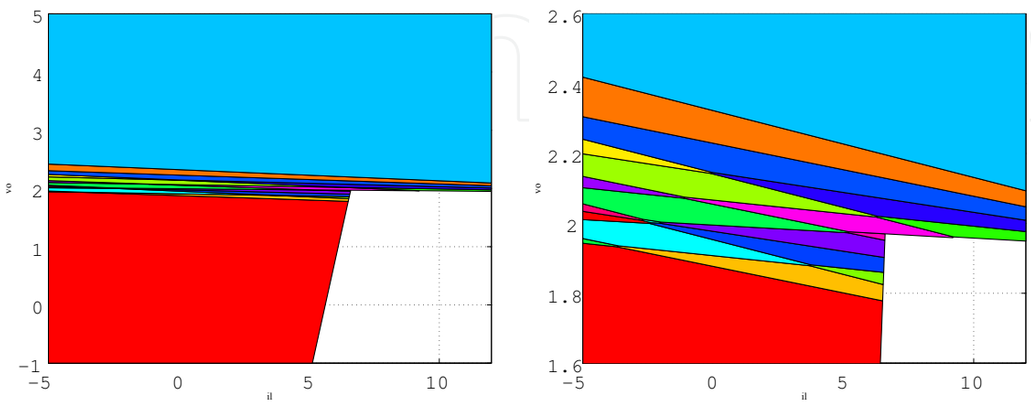

Fig. 2. State partition for $N_p = 5$ (left: whole, rigtht: closeup).

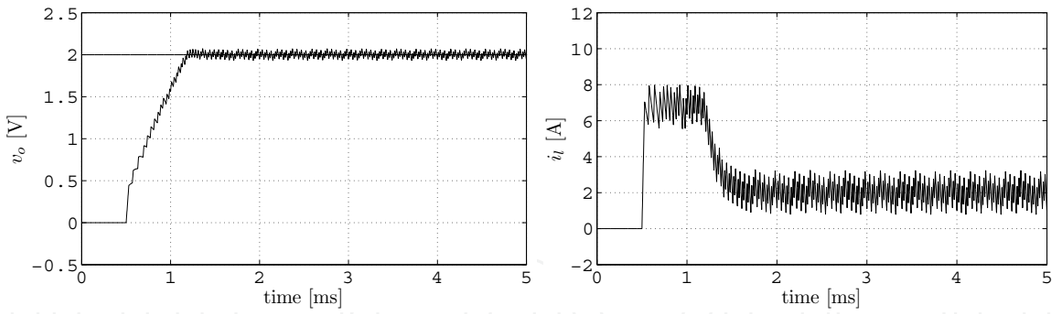

Fig. 3. Simulation result in case computation delay is negligible for $N_p = 3$ (left: v_o, right: i_l).

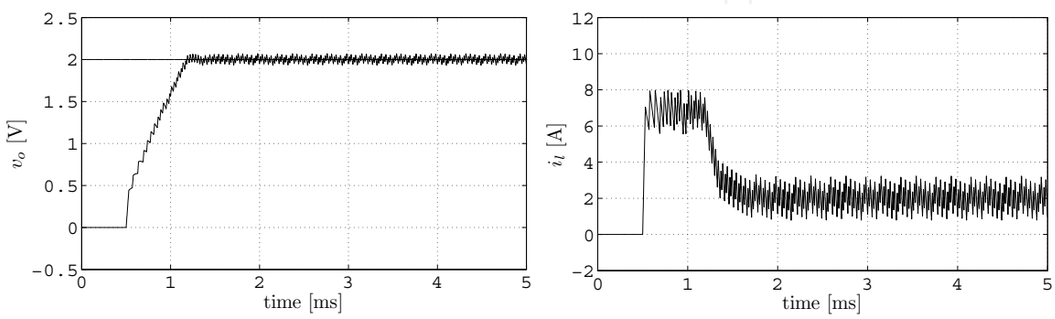

Fig. 4. Simulation result in case computation delay is negligible for $N_p = 5$ (left: v_o, right: i_l).

the two outputs shown in Figs. 3 and 4. In other words, the performance is almost identical for $N_p = 3$ and $N_p = 5$ as long as the computation time is minimal.
On the other hand, as described later in the next section, the computation time should be considered. because of the effects of various factors such as DSP performance and the number of state partitions. In preliminary experiments, 5 [μs] and 8 [μs] for $N_p = 3$ and $N_p = 5$, respectively, are obtained as average computation delay. Using the values, we set the delay for determination of the switching signal after measurement of the state in the simulation. Figs. 5 and 6 illustrate the simulation results under the assumption that the computation delay is not negligible, i.e., the delay is assumed to exist for the computation. From Figs. 5 and 6, the switching intervals that exceed 20[¯s] can be seen. Thus, the ripple effect increases as the

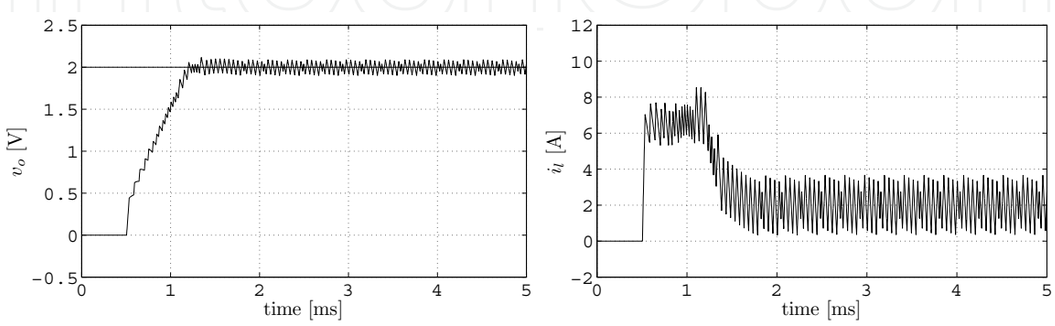

Fig. 5. Simulation result in case computation delay is 5 [μs] for $N_p = 3$ (left: v_o, right: i_l).

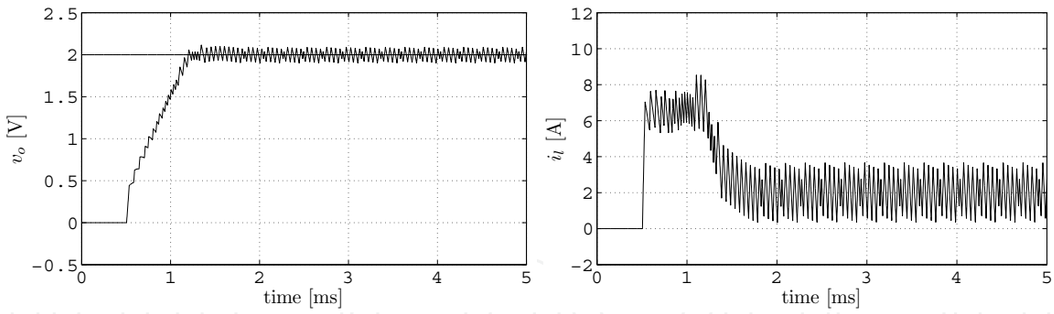

Fig. 6. Simulation result in case computation delay is 8 [μs] for $N_p = 5$ (left: v_o, right: i_l).

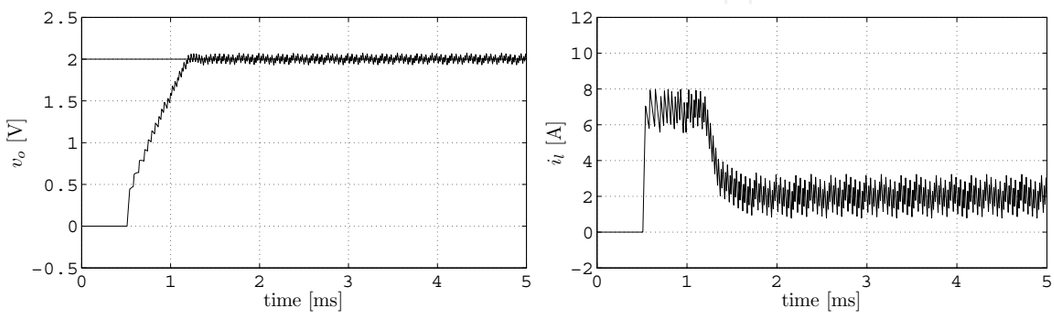

Fig. 7. Simulation result with consideration of computation time for $N_p = 5$ (left: v_o, right: i_l).

difference widens between the value of the measured state and that of the input which is determined after the delay.

3.3 Modification of control method

In the method proposed(21) in the Appendix, input is applied after examination of the region in which the state belongs. However, as mentioned above, the performance is not necessarily satisfactory due to the computation delay even if the horizon is small. Therefore, the control method should be slightly modified in order to consider the computation delay so that performance is not degraded. Specifically, instead of the first one, the second element of the optimal input sequence is applied to the system at the beginning of the next control period. In addition, the first element of the optimal input sequence has to be used as that given at the last sampling. In other words, the first element is not solved but is set as that given at the last period, i.e., in the modified control method, δ_0 and z_0 in Eqs. (20) and (21), respectively, are given in advance as the constants of the last optimized input sequence, not solved as the optimized variables. Note that the modified control method requires $N_p > 1$ due to the structure. Fig. 7 depicts the simulation result by the modified method above mentioned. Compared with Fig. 6, the result shown in Fig. 7 is improved in the sense that the ripple is reduced in steady state.

4. Experimental result

In this section, we show the effectiveness of the modified proposed method(21) through experiments. In addition, the effectiveness for consideration of the switching loss is demonstrated.

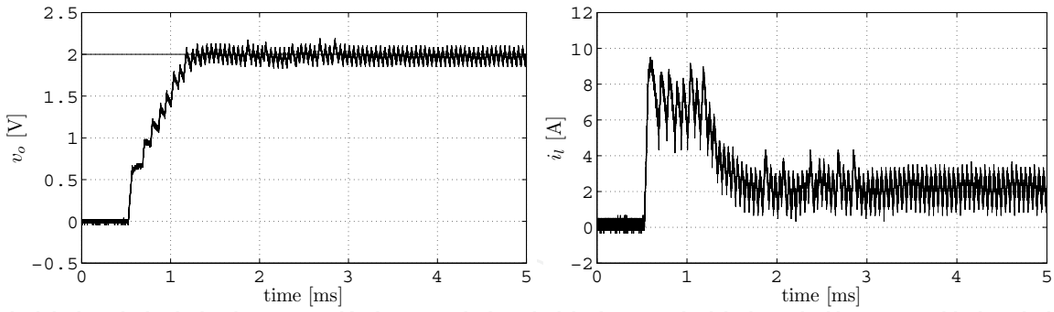

Fig. 8. Experimental result without consideration of computation delay (left: v_o, right: i_l).

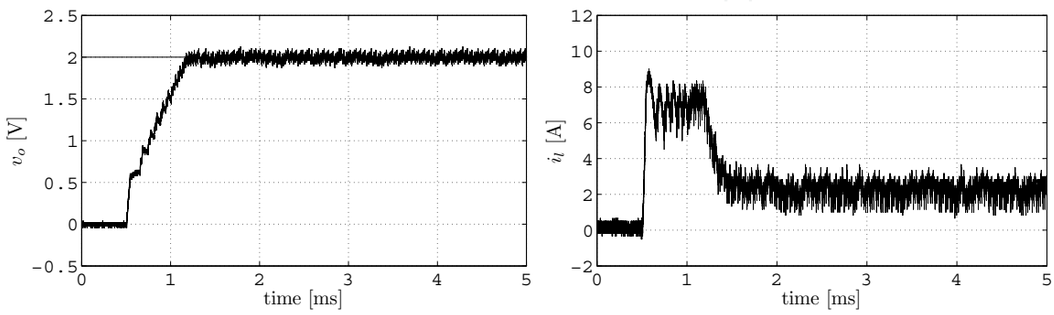

Fig. 9. Experimental result with consideration of computation delay (left: v_o, right: i_l).

The experiments are carried out on a DSP (Texas Instruments TMS3200C/F2812, operating frequency: 150 [MHz], AD-converter: 12 [bit], conversion time: 80 [ns]).

4.1 Comparison of proposed method(21) and its modified method

Fig. 8 shows the experimental result obtained without considering the computation delay for state distinction for $N_p = 5$. Similar to simulation results shown in Fig. 4, many switchings are described with intervals exceeding 20 [μs] although the control period is 10 [μs]. The reason for the results is that the state transits to another which is not the predictive one, due to the computation delay. Therefore, the computation delay for state distinction should be considered in the experiments. Fig. 9 shows the experimental result upon consideration of the computation delay. Note that the results shown in Fig. 9 are obtained by the modified control method mentioned in the previous section.
Compared with the results shown in Fig. 8, the ripple effect is reduced as shown in Fig. 9. This reduction occurs because the computation delay is considered in the latter result. Thus, the effectiveness of the modified control method in Subsection 3.3 is demonstrated.

4.2 Consideration of switching loss

The shorter the control period, the more the switching losses tend to increase, as do the number of switchings. In the proposed method, the switching loss can be considered by incorporating it into the cost function. This can be achieved by setting $Q = qI_{N_p-1}$ where $q = 10^{-3}$ in Eq. (42). The experimental result is shown in Fig. 10. From Fig. 10, the output voltage is tracked to the voltage reference even though the term to reduce switching is added into the cost function. Fig. 10 also shows that the inductor current does not severely exceed the limit

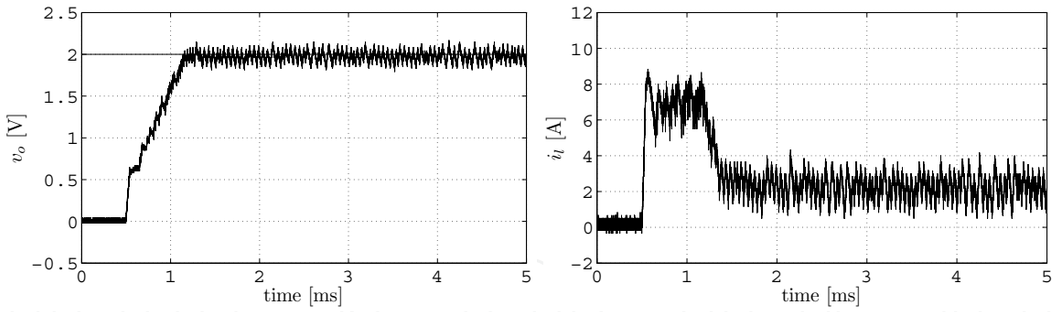

Fig. 10. Experimental result with consideration of computation delay and the switching loss for $N_p = 5$ (left: v_o, right: i_l).

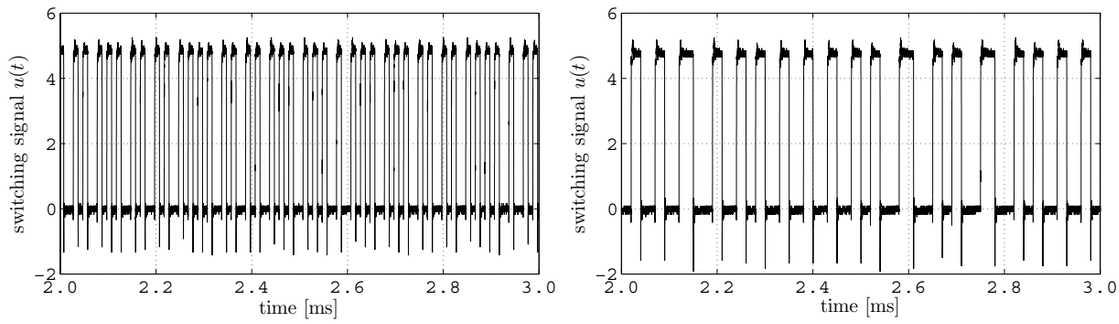

Fig. 11. Experimental result of switching signal without/with consideration of the switching loss for $N_p = 5$ (left: without, that in Fig. 9, right: with, that in Fig. 10).

of 8 [A]. Fig. 11 shows the switching signals for Figs. 9 and 10. From the right of Fig. 11, the switching frequency is reduced by considering the switching loss in the cost function given by Eq. (45). Thus, both tracking performance and switching loss can be considered simultaneously in the proposed method.

5. Conclusions

In this paper, a novel control method for the dc-dc converter has been proposed. The dc-dc converter has been modeled as a mixed logical dynamical (MLD) system since it has the ability to combine continuous and discrete properties. For the control, a model predictive control (MPC) based method has been introduced. The optimization problem has been solved as a multi-parametric off-line programming problem. The result has been obtained as the state space partition which makes the implementation feasible. As a result, computation time is shortened without deteriorating control performance. Finally, it has been demonstrated that the output voltage has been tracked to the reference at the expense of tracking performance by introducing the term to reduce the switching in the cost function. In some cases, other factors such as resistance loss in r_l shown in Fig. 1 may need to be considered, although the cost function given by Eq. (28) considers only the tracking performance and switching loss. Note, however, that the factors represented as linear and/or quadratic forms of the state variable can be incorporated into the cost function.
Further research includes robustness analysis in implementation and investigation of performance for different cost functions as mentioned above.

Acknowledgment

We are grateful to the Okasan-Kato Foundation. We also thank Professor Manfred Morari, Ph.D, Sébastien Mariéthoz, Ph.D, Andrea Beccuti, Ph.D, of ETH Zurich for valuable comments and suggestions.

Here, the proposed method(15) is reviewed in brief.

MIQP derives the values that minimize an estimation of a given cost function under constraints given by inequalities and/or equalities concerning integer variables. The MIQP for Eqs. (14) to (16) is given as follows.

$$\min_{\nu_t} \ \nu_t' S_1 \nu_t + 2(S_2 + x(t)' S_3)\nu_t, \tag{23}$$

$$\text{subject to } F_1 \nu_t \leq F_2 + F_3 x(t), \tag{24}$$

where ν_t is

$$\nu_t = \begin{bmatrix} \Delta_t' & \Xi_t' \end{bmatrix}', \tag{25}$$

$$\Delta_t = \begin{bmatrix} \delta(0|t) & \dots & \delta(N_p - 1|t) \end{bmatrix}', \tag{26}$$

$$\Xi_t = \begin{bmatrix} z(0|t) & \dots & z(N_p - 1|t) \end{bmatrix}'. \tag{27}$$

To derive the optimal input sequence for Eqs. (14) to (16), the following cost function is set.

$$\begin{aligned} J(x(t), \Delta_t, \Xi_t) = &\sum_{k=1}^{N_p} \| y(k|t) - v_{\text{ref}} \|_2^2 \\ &+ \Delta_t' \tilde{H} \Delta_t + 2L\Delta_t, \end{aligned} \tag{28}$$

where v_{ref} denotes the constant voltage reference. In Eq. (28), the first term is associated with the tracking performance whereas the switching loss can be also considered in the second and third terms. Eq. (28) is rewritten as the general MIQP form of Eqs. (23) in order to solve the minimization problem. By Eqs. (14) and (15), $y(k|t)$ which is the predictive output k steps ahead of t is described as follows.

$$\begin{aligned} y(k|t) &= C(A^k x(t) + \sum_{j=0}^{k-1} A^{k-j-1} B z(j)) \\ &= C(A^k x(t) + G_k \Xi_k), \end{aligned} \tag{29}$$

where $G_k = \begin{bmatrix} A^{k-1}B & A^{k-2}B & \dots & B \end{bmatrix}$. By substituting Eq. (29) for Eq. (28), the minimization problem for Eq. (28) is formalized as follows.

$$\begin{aligned} \min_{\Delta_t, \Xi_t} \Bigg(&\sum_{k=1}^{N_p} \Xi_t' G_k' C' C G_k \Xi_t - 2 \sum_{k=1}^{N_p} v_{\text{ref}}' C G_k \Xi_t \\ &+ 2 \sum_{k=1}^{N_p} x(t)' A'^k C' C G_k \Xi_t + \Delta_t' \tilde{H} \Delta_t + 2L\Delta_t \Bigg). \end{aligned} \tag{30}$$

Note that the irrelative terms for the minimization problem are omitted in Eq. (30). Connected with Eq. (23), the optimization problem of Eq. (30) is transformed as

$$\min_{\Delta_t, \Xi_t} \begin{bmatrix} \Delta_t \\ \Xi_t \end{bmatrix}' S_1 \begin{bmatrix} \Delta_t \\ \Xi_t \end{bmatrix} + 2(S_2 + x(t)' S_3) \begin{bmatrix} \Delta_t \\ \Xi_t \end{bmatrix}, \tag{31}$$

where S_1, S_2 and S_3 are,

$$S_1 = \begin{bmatrix} \tilde{H} & O \\ O & \sum_{k=1}^{N_p} G_k' C' C G_k \end{bmatrix} \in \mathbb{R}^{2N_p \times 2N_p}, \tag{32}$$

$$S_2 = \begin{bmatrix} L & -\sum_{k=1}^{N_p} v_{\text{ref}}' C G_k \end{bmatrix} \in \mathbb{R}^{1 \times 2N_p}, \tag{33}$$

$$S_3 = \begin{bmatrix} O & \sum_{k=1}^{N_p} A_k' C' C G_k \end{bmatrix} \in \mathbb{R}^{2 \times 2N_p}, \tag{34}$$

respectively.
Let us rewrite the constraint as the general form like inequality (24). Recall that only two discrete inputs are permitted in the considered system. The constraint represented by Eq. (9) is also transformed as

$$\tilde{F}_1 \begin{bmatrix} \Delta_t \\ \Xi_t \end{bmatrix} \leq \tilde{F}_2 + \tilde{F}_3 x(t), \tag{35}$$

where $\tilde{F}_1$, $\tilde{F}_2$ and $\tilde{F}_3$ are, respectively,

$$\begin{aligned} \tilde{F}_1 &= \begin{bmatrix} E_1 & & O & E_2 & & O \\ & \ddots & & & \ddots & \\ O & & E_1 & O & & E_2 \end{bmatrix} \in \mathbb{R}^{4N_p \times 2N_p}, \\ \tilde{F}_2 &= \begin{bmatrix} E_5 \\ \vdots \\ E_5 \end{bmatrix} \in \mathbb{R}^{4N_p}, \quad \tilde{F}_3 = \begin{bmatrix} E_4 & E_4 \\ \vdots & \vdots \\ E_4 & E_4 \end{bmatrix} \in \mathbb{R}^{4N_p \times 2}. \end{aligned} \tag{36}$$

The constraints imposed on the inductor current limitation is are necessary to prevent damage to the switching device from excessive current. More specifically, if the predictive inductor current at $t+1$, i.e., $i_l(1|t)$, exceeds its limit, $i_{l,\max}$, then the switch is forced to be off. Such an additional condition can be described as

$$[i_l(1|t) > i_{l,\max}] \rightarrow [\delta(0) = 0]. \tag{37}$$

Transformed into the inequality, Eq. (37) is described as

$$i_l(1|t) - i_{l,\max} \leq M(1 - \delta(0)), \tag{38}$$

where M is the admissible upper limit of i_l. Since $x = \begin{bmatrix} i_l & v_o \end{bmatrix}'$, replaced the first row of A and the first element of B with A_1 and b_1, respectively, $i_l(1|t)$ is recast as,

$$i_l(1|t) = \begin{bmatrix} a_{11} & a_{12} \end{bmatrix} x(t) + b_1 z(0), \tag{39}$$

where $\begin{bmatrix} a_{11} & a_{12} \end{bmatrix}$ is the first row of A. Consequently, using Eq. (39), inequality (38) can be expressed as

$$M\delta(0) + b_1 z(0) \leq (M + i_{l,\max}) - \begin{bmatrix} a_{11} & a_{12} \end{bmatrix} x(t). \tag{40}$$

Add Eq. (40) as a new constraint to the last row of Eq. (36), then Eq. (36) is modified as follows.

$$F_1 = \begin{bmatrix} & & & & \tilde{F}_1 & & & \\ M & 0 & \dots & 0 & b_1 & 0 & \dots & 0 \end{bmatrix}', \quad F_2 = \begin{bmatrix} \tilde{F}_2 \\ M + i_{l,\max} \end{bmatrix}, \; F_3 = \begin{bmatrix} \tilde{F}_3 \\ A_1 \end{bmatrix}. \tag{41}$$

The switching loss can also be considered in the second and third terms in Eq. (28). In Eq. (28), for example, $L = O$ and $\tilde{H}$ is set with $Q \succeq 0$ as follows.

$$\tilde{H} = (\Pi_1 - \Pi_2)' Q (\Pi_1 - \Pi_2), \tag{42}$$

where Π_1 and Π_2 are, respectively,

$$\Pi_1 = \begin{bmatrix} 0 & \\ \vdots & I_{N_p-1} \\ 0 & \end{bmatrix} \in \mathbb{R}^{(N_p-1)\times N_p}, \tag{43}$$

$$\Pi_2 = \begin{bmatrix} & 0 \\ I_{N_p-1} & \vdots \\ & 0 \end{bmatrix} \in \mathbb{R}^{(N_p-1)\times N_p}. \tag{44}$$

Note that when $\tilde{H}$ and L are set above, the estimation of the cost function of Eq. (28) increases in response to the number of switchings required. Therefore, the switching loss can be reduced depending on Q in Eq. (42).

If the cost function is described, the optimal input sequence can be derived. However, it is impractical to apply it to the considered dc-dc converter with a short control period since the computation requires much solution time for every control period. Then, the method above is transformed into mp-MIQP so that solving the optimization problem on-line is no longer necessary. Eq. (28) is adopted as the cost function again for mp-MIQP. Then, Eq. (28) is described as follows.

$$\begin{aligned} & J(x, \Delta, \Xi) \\ &= \sum_{k=1}^{N_p} \Xi' G_k' C' C G_k \Xi + 2 \sum_{k=1}^{N_p} x' A'^k C' C G_k \Xi \\ &\quad + \sum_{k=1}^{N_p} x' A'^k C' C A^k x - 2 \sum_{k=1}^{N_p} v_{\mathrm{ref}}' C G_k \Xi \\ &\quad - 2 \sum_{k=1}^{N_p} v_{\mathrm{ref}}' C A^k x + \Delta' \tilde{H} \Delta + 2 L \Delta, \end{aligned} \tag{45}$$

where $\Delta = \begin{bmatrix} \delta_0 & \dots & \delta_{N_p-1} \end{bmatrix}$ and $\Xi = \begin{bmatrix} z_0 & \dots & z_{N_p-1} \end{bmatrix}$. Associated with Eq. (17), the optimization problem of Eq. (45) is transformed as follows.

$$\begin{aligned} \min_{\Delta,\Xi} \; & \begin{bmatrix} \Delta \\ \Xi \end{bmatrix}' H \begin{bmatrix} \Delta \\ \Xi \end{bmatrix} + 2x' F \begin{bmatrix} \Delta \\ \Xi \end{bmatrix} + x' Y x \\ & + 2 C_f \begin{bmatrix} \Delta \\ \Xi \end{bmatrix} + 2 C_x x, \end{aligned} \tag{46}$$

where $\tilde{H} = S_1$, $F = S_3$ and $C_f = S_2$, respectively. Note that there exists a clear difference between notations of ν_t and ν. The former is utilized for MIQP while the latter is used for mp-MIQP. The others are

$$Y = \sum_{k=1}^{N_p} A'^k C' C A^k, \tag{47}$$

$$C_x = -\sum_{k=1}^{N_p} v'_{\text{ref}} C A^k. \tag{48}$$

The constraints are given by

$$F_1 \begin{bmatrix} \Delta \\ \Xi \end{bmatrix} \leq F_2 + F_3 x. \tag{49}$$

Transformed as above, the optimization problem is solved offline as mp-MIQP. Then, the result is employed for on-line control.

6. References

[1] *Hybrid systems* I, II, III, IV, V, Lecture Notes in Computer Science, 736, 999, 1066, 1273, 1567, New York, Springer-Verlag, 1993 to 1998.

[2] "Special issue on hybrid control systems," *IEEE Trans. Automatic Control*, Vol. 43, No. 4, 1998.

[3] "Special issue on hybrid systems," *Automatica*, Vol. 35, No. 3, 1999.

[4] "Special issue on hybrid systems," *Systems & Control Letters*, Vol. 38, No. 3, 1999.

[5] "Special issue hybrid systems: Theory & applications", *Proc. IEEE*, Vol. 88, No. 7, 2000.

[6] T. Ushio, "Expectations for Hybrid Systems," *Systems, Control and Information*, Vol. 46, No. 3, pp. 105–109, 2002.

[7] S. Almer, H. Fujioka, U. Jonsson, C. Y. Kao, D. Patino, P. Riedinger, T. Geyer, A. G. Beccuti, G. Papafotiou, M. Morari, A. Wernrud and A. Rantzer, "Hybrid Control Techniques for Switched-Mode DC-DC Converters Part I: The Step-Down Topology," *Proc. ACC* , pp. 5450–5457, 2007.

[8] A. G. Beccuti, G. Papafotiou, M. Morari, S. Almer, H. Fujioka, U. Jonsson, C. Y. Kao, A. Wernrud, A. Rantzer, M. Baja, H. Cormerais, and J. Buisson, "Hybrid Control Techniques for Switched-Mode DC-DC Converters Part II: The Step-Up Topology," *Proc. ACC*, pp. 5464–5471, 2007.

[9] A. G. Beccuti, G. Papafotiou, R. Frasca and M. Morari, "Explicit Hybrid Model Predictive Control of the dc-dc Boost Converter," *Proc. IEEE PESC*, pp. 2503–2509, 2007.

[10] I. A. Fotiou, A. G. Beccuti and M. Morari, "An Optimal Control Application in Power Electronics Using Algebraic Geometry," *Proc. ECC*, pages 475–482, July 2007.

[11] R. R. Negenborn, A. G. Beccuti, T. Demiray, S. Leirens, G. Damm, B. D. Schutter and M. Morari, "Supervisory Hybrid Model Predictive Control for Voltage Stability of Power Networks," *Proc. ACC*, pp. 5444–5449, 2007.

[12] A. G. Beccuti, G. Papafotiou and M. Morari, "Optimal control of the buck dc-dc converter operating in both the continuous and discontinuous conduction regimes," *Proc. IEEE CDC*, pp. 6205–6210, 2006.

[13] T. Geyer, G. Papafotiou, M. Morari, “On the Optimal Control of Switch-Mode DC-DC Converters," *Hybrid Systems: Computation and Control*, Vol. 2993, pp. 342–356, Lecture Notes in Computer Science, 2004.
[14] G. Papafotiou, T. Geyer, M. Morari, “Hybrid Modelling and Optimal Control of Switch-mode DC-DC Converters," *IEEE Workshop on Computers in Power Electronics (COMPEL)*, pp. 148–155, 2004.
[15] K. Asano, K. Tsuda, A. Bemporad, M. Morari, “Predictive Control for Hybrid Systems and Its Application to Process Control," *Systems, Control and Information*, Vol. 46, No. 3, pp. 110–119, 2002.
[16] M. Ohshima, M. Ogawa, “Model Predictive Control –I– Basic Principle: history & present status," *Systems, Control and Information*, Vol. 46, No. 5, pp. 286–293, 2002.
[17] M. Fujita, M. Ohshima, “Model Predictive Control –VI– Model Predictive Control for Hybrid Systems," *Systems, Control and Information*, Vol. 47, No. 3, pp. 146–152, 2003.
[18] F. Borrelli, M. Baotic, A. Bemporad, M. Morari, “An efficient algorithm for computing the state feedback optimal control law for discrete time hybrid systems," In *Proc. ACC*, pp. 4717–4722, 2003.
[19] A. Bemporad, M. Morari, “Control of systems integrating logic, dynamics, and constraints," *Automatica*, Vol. 35, No. 3, pp. 407–427, 1999.
[20] M. Kvasnica, P. Grieder, M. Boatić and F. J. Christophersen, “Multi-Parametric Toolbox (MPT)," Institut für Automatik, 2005.
[21] N. Asano, T. Zanma and M. Ishida, “Optimal Control of DC-DC Converter using Mixed Logical Dynamical System Model," *IEEJ Trans. IA*, Vol. 127, No. 3, pp. 339–346, 2007.

Model Predictive Control

Edited by Tao Zheng

ISBN 978-953-307-102-2

Hard cover, 304 pages

Publisher Sciyo

Published online 18, August, 2010

Published in print edition August, 2010

Frontiers of Model Predictive Control Robust Model Predictive Control Nonlinear Model Predictive Control Excellent Applications Guide for Researchers and Engineers Recent Achievements of Authors over the World Theory with Practical Examples Kinds of Algorithms for Choice

INTECH
open science | open minds

InTech Europe

University Campus STeP Ri
Slavka Krautzeka 83/A
51000 Rijeka, Croatia
Phone: +385 (51) 770 447
Fax: +385 (51) 686 166
www.intechopen.com

InTech China

Unit 405, Office Block, Hotel Equatorial Shanghai
No.65, Yan An Road (West), Shanghai, 200040, China
中国上海市延安西路65号上海国际贵都大饭店办公楼405单元
Phone: +86-21-62489820
Fax: +86-21-62489821

IntechOpen